A method for real-time compensation of magnetometers embedded on smartphones

Pasquale Daponte, Luca De Vito, Francesco Picariello, Sergio Rapuano, Carmine Sementa
Department of Engineering, University of Sannio, Benevento, Italy
Email: {daponte, devito, fpicariello, rapuano, csementa}@unisannio.it

***Abstract*—This paper deals with a real-time compensation method of long term time-variant disturbances for magnetometers embedded on smartphones. The proposed method compensates the effect of long term time-variant disturbances, continuously, using a least-square ellipsoid-based compensation procedure. In this paper, the proposed method is described and its advantages respect to the methods available in literature are highlighted. Furthermore, preliminary simulation tests have been performed and the obtained results reported.**

I. Introduction

MicroElectroMechanical Systems (MEMS) are sensors or actuators that combine technologies related to microelectronics and micro-mechanical structures. MEMS is the most common technology used for the development of accelerometers, gyroscopes and magnetometers. These three sensors together form a Magnetic Angular Rate Gravity sensor module (MARG). MARG sensors are used especially for navigation applications as Inertial Navigation Systems (INSs).

Nowadays, smartphones embed MARG sensors. For this reason, smartphones are used for indoor and outdoor navigation applications [1]. In literature, indoor positioning techniques have been widely analyzed and several solutions provided. These solutions are oriented to support automatic guidance for visitors in public buildings such as museums, galleries, etc. For example in [2], the authors propose an indoor positioning system using a Pedestrian Dead Reckoning (PDR) algorithm and an error-tolerant magnetic map matching algorithm. The PDR algorithm allows to measure the number of steps, the stride length and direction of pedestrian using the data provided by the MARG embedded on smartphone. On the other hand, the magnetic map matching algorithm allows to identify the pedestrian position by knowing the magnetic features of different indoor positions. In this way, if the magnetic map of specific indoor environment is known, it is possible to determine the position by measuring the magnetic distortions. For outdoor navigation, GPS data and MARG measurements are used to determine position and orientation of the smartphone, respectively. In particular, MEMS accelerometers can be used to determine the current state of the user, e.g. standing, walking, or fast moving in a car or public transportation. In addition, the magnetometer provides orientation of movements. The measurement of these sensors can be used for dead reckoning in case of GPS data not available. In [3], the authors investigate the use of GPS and MARG for navigation applications comparing the performance of four different smartphones in terms of localization and orientation measurement accuracies. During the test, indoor and outdoor environments in urban areas are considered. As expected, the performance of the different smartphones in outdoor environments is better than indoor ones. However, in both of the environments, the main drawback is the disturbance of nearby metallic objects on the magnetic field measurements. The magnetometer provides subject navigation direction measurements by measuring the Earth magnetic field. Local magnetic field is normally distorted by disturbances due to the presence of ferromagnetic materials and electromagnetic sources in the environment. These disturbances change during the navigation and affect the magnetic field measurements. Since the mobility of the subject carrying the sensor is not constrained, the sensing disturbances can be generally time-variant. For example in [4], this kind of sensors is used in home rehabilitation applications where the subject mobility should not be constrained. Indeed, in this case, the subjects are allowed to move around likely getting close to disturbance sources (i.e. appliances) that are present in a typical home environment. For this reason, in order to reduce the effect of these disturbances on magnetometer measurements, it is necessary to implement continuous compensation procedures. According to [5], these compensation procedures can be classified in: (i) methods requiring measurements provided by another measurement system, (ii) and methods using the measurements provided by the magnetometer itself. For example in [5], the authors propose a magnetometer compensation algorithm by applying a neural network. The neural network aims to compensate the magnetometer errors due to magnetic field disturbances by estimating during the training step the relationship between the measurements provided by the magnetometer and those provided by the GPS. When the magnetometer becomes the primary sensor, the trained neural network is used to correct the measurements. This technique has several disadvantages: (i) it requires the use of the GPS module embedded on smartphone increasing the power consumption of the entire system, (ii) the neural network algorithm has a high computational complexity, and (iii) the proposed method estimates the compensation parameters only when the GPS data are available. On the other hand, a method based on the magnetometer measurements using an unscented Kalman filter is proposed in [6]. In this case, the method allows to compensate the effect of disturbances estimating the setting parameters of

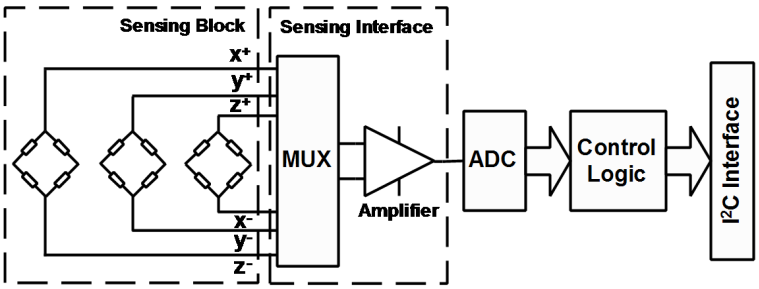

Fig. 1. Architectural overview of the magnetometer embedded in the LSM303DLH sensor module [7].

the magnetometer continuously. The main drawback of this technique is that for unscented and extended Kalman filters, a linearization of the non-linear functions describing the variations of each compensation parameter is implemented. This approximated functions are valid for small variations of the setting parameters. Thus, this method is used when the setting parameters have a low variability [6].

In this paper, a real-time compensation method based on the nine-parameter magnetometer error model is proposed. This method allows the estimation of the compensation model parameters in case of long term time-variant disturbances and large magnetic field variations. The first simulation results are presented and discussed. The paper is organized as it follows. In Section II, a description of the nine-parameter magnetometer error model already available in literature is reported. A performance evaluation of ellipsoid-based compensation techniques is presented in Section III. Section IV describes the proposed real-time compensation method and the first simulation results are reported in Section V.

II. Magnetometer error model

In [7], the sensor module consisting of a 3-axis accelerometer and 3-axis magnetometer provided by ST-Microelectronics and usually embedded on smartphones is described. The block diagram of this sensor module is reported in Fig. 1. It consists of: (i) a sensing block, (ii) a sensing interface, (iii) an Analog to Digital Converter (ADC), (iv) a control logic, and (v) and a digital interface (i.e. I^2C). The sensing block consists of capacitive transducers for the measurement of the gravity acceleration and of magneto-resistances used for the measurement of the Earth magnetic field. The voltage signals provided by the sensing block are amplified by the sensing interface and digitized by means of the ADC. The digital values are sent to the smartphone application processor via a digital interface.

For the measurement of the Earth magnetic field, Anisotropic Magneto-Resistances (AMRs) are used as components of three Wheatstone bridges. An AMR is a resistor that changes its resistance value according to the magnetic field surrounding the sensor [8]. The sensitivity to the incident magnetic field depends on its angle of incidence. In this way, it is possible to discriminate the effect of the external magnetic field along the axis of the AMR. In order to convert the resistance variation in a voltage signal, a Wheatstone bridge containing four AMRs is used. By using three orthogonal AMR Wheatstone bridges, it is possible to measure the magnetic field in three dimensions [8]. The operating principle of an AMR Wheatstone bridge requires that the four AMRs are equal. In this case in presence of no magnetic field, the voltage output of the Wheatstone bridge should be equal to zero. As described in [8], due to the manufacturing limits, the four AMRs have slightly different measurement characteristics. These differences are the cause of the following measurement errors: (i) offset errors, (ii) sensitivity errors, and (iii) cross-axis sensitivity errors. The offset errors are related to the bridge voltage offsets on the three-axis signals when no magnetic field is applied on the sensor. In this case, it is necessary to compensate for the bridge offset just once. A method used for the offset compensation is based on Helmholtz coils. Helmholtz coils allow to apply on the sensor under test a known magnetic field. By deleting the Earth magnetic field with the magnetic field provided by the coils, it is possible to measure the voltage offsets on each sensor axis. An alternative method is to measure the sensor output at different orientations assuming that the applied field is constant. In this way, by using multiple observations, a least squares approach can be used to solve for offset estimation. Analogously, multiple observations turn out viable to estimate the values of the other measurement errors as the sensitivity of an AMR changes according to the sensed field magnitude, resulting in scale factor errors, and its potentially uneven magnetization may change the cross-axis sensitivity. All these errors can be modeled with a scale factor matrix, a non-orthogonality matrix and an offset vector [8] as follows:

$$\mathbf{h_m} = \mathbf{SCh} + \mathbf{b_0} \tag{1}$$

where $\mathbf{h_m}$ is the magnetic field vector measured by the sensor, $\mathbf{h}$ is the Earth magnetic field vector, $\mathbf{S}$ is the scale factor matrix with s_x, s_y, and s_z standing for the scale factors for each sensor axis:

$$\mathbf{S} = \begin{pmatrix} s_x & 0 & 0 \\ 0 & s_y & 0 \\ 0 & 0 & s_z \end{pmatrix} \tag{2}$$

C is the non-orthogonality matrix defined as:

$$\mathbf{C} = \begin{pmatrix} \epsilon_{\mathbf{x}} & \epsilon_{\mathbf{y}} & \epsilon_{\mathbf{z}} \end{pmatrix}^{-1} \tag{3}$$

where $\epsilon_{\mathbf{x}}$, $\epsilon_{\mathbf{y}}$, and $\epsilon_{\mathbf{z}}$ are vectors that describe the $\mathbf{x}$, $\mathbf{y}$ and $\mathbf{z}$ Wheatstone bridges attitudes respectively in the sensor frame. The offset error vector $\mathbf{b_0}$ takes into account an offset error related to each sensor axis (b_{x_0}, b_{y_0}, and b_{z_0}):

$$\mathbf{b_0} = \begin{pmatrix} b_{x_0} & b_{y_0} & b_{z_0} \end{pmatrix}^T \tag{4}$$

In addition to errors due to manufacturing, magnetic field sensors also suffer errors related to magnetic perturbations. The presence of ferromagnetic materials and electromagnetic systems in the proximity of the sensor are the main causes of these perturbations. These perturbations are classified in hard and soft iron perturbations. Hard iron magnetism is the magnetic field produced by permanent magnet and electrical equipment [9], usually placed on the sensor platform. Consequently, the hard iron magnetic field contribution is expressed in the sensor frame. This error can be modeled as offset contribution on the values measured by each sensor axis:

$$\mathbf{b_m} = \begin{pmatrix} b_{x_m} & b_{y_m} & b_{z_m} \end{pmatrix}^T \tag{5}$$

Soft-iron magnetism is produced by materials that distort the underlying magnetic field, changing the magnitude as well as the direction of the sensed field [9]. In this case, a 3 by 3 matrix can be used to model this error, as follows:

$$\mathbf{A} = \begin{pmatrix} a_{xx} & a_{xy} & a_{xz} \\ a_{xy} & a_{yy} & a_{yz} \\ a_{xz} & a_{yz} & a_{zz} \end{pmatrix} \tag{6}$$

By combining both manufacturing errors (1) and magnetic perturbation errors (5) and (6), it is possible to evaluate the complete error model for the 3-axis magnetometer:

$$\mathbf{h_m} = \mathbf{SC}(\mathbf{Ah} + \mathbf{b_m}) + \mathbf{b_0} \tag{7}$$

This equation can be simplified as follows:

$$\mathbf{h_m} = \mathbf{Mh} + \mathbf{b} \tag{8}$$

where $\mathbf{M} = \mathbf{SCA}$ and $\mathbf{b} = \mathbf{SCb_m} + \mathbf{b_0}$.
For navigation applications, the matrix $\mathbf{M}$ and the vector $\mathbf{b}$ change continuously according to the variations of magnetic perturbations due to hard and soft iron effects in the environment. To this aim, the proposed compensation method allows the estimation of these two quantities, $\mathbf{M}$ and $\mathbf{b}$, continuously. In this way, it is possible to compensate, in real-time, the effect on measurements of magnetic field time-variant disturbances.

III. Ellipsoid-based compensation method

The proposed compensation method is based on the already known ellipsoid compensation one [10]. In this case, by using a set of measurements collected at different static sensor orientations $\mathbf{h_m} = \{\mathbf{h_{m1}}, \mathbf{h_{m2}}, ..., \mathbf{h_{mn}}\}$ and considering the magnitude of the measured magnetic field constant at each sensor orientation, it is possible to evaluate the magnetometer model parameters. Normally in literature, the magnitude of the Earth magnetic field is assumed equal to unity, without loss of generality. According to (8), this constraint can be expressed with the following equation:

$$(\mathbf{h_m} - \mathbf{b})^T {\mathbf{M_{inv}}}^T \mathbf{M_{inv}} (\mathbf{h_m} - \mathbf{b}) - 1 = 0 \tag{9}$$

where $\mathbf{M_{inv}} = \mathbf{M}^{-1}$.
The equation (9) describes a generic ellipsoid. Several methods can be used for solving (9) respect to the matrix $\mathbf{M_{inv}}$ and the vector $\mathbf{b}$. These methods are classified according to [10] in 3-D ellipsoid fitting via: (i) non-linear optimization, (ii) linear optimization, and (iii) enclosing ellipsoid. In the first case, iterative methods (such as Newton-Rhapson) are used to solve directly the non-linear equation (9). These methods require the implementation of computationally expensive algorithms. On the other hand, (9) can be rewritten in a linear form by considering small variations for $\mathbf{M_{inv}}$ and $\mathbf{b}$. In this case, the algorithm can be simplified but it is not valid for navigation applications where magnetic perturbations provide big variation of the setting parameters. Another procedure is based on finding the Minimum-Volume Enclosing Ellipsoid (MVEE) of the sensor measurements [10].
The method proposed in this paper is based on the least-square non linear optimization method. This optimization method consists of a minimization criterion, which can be formulated as follows:

$$\{\mathbf{M_{est}}, \mathbf{b_{est}}\} = \arg \min_{(\mathbf{M},\mathbf{b})} \sum_{n=1}^{N} (||\mathbf{M_{inv}}(\mathbf{h_{mn}} - \mathbf{b})||^2 - 1)^2 \tag{10}$$

According to (10), the compensation procedure requires the orientation of the sensor in N positions for measuring the h_{mn} at several orientations. The performance of this compensation procedure depends on several parameters: (i) the 3D spatial distribution of the orientations used during the compensation procedure, (ii) the number of orientations N considered for the sensor compensation (minimum 9 different orientations), (iii) the Signal to Noise Ratio (SNR) on the measurement signals, and (iv) the number of samples P to acquire at each orientation. The 3D spatial distribution of the orientations used for the compensation procedure affects directly the compensation results. In particular, the more uniformly distributed the orientations considered in the compensation are in the 3D space, the less the error referred to each estimated compensation parameter. Thus, for the proposed real-time method, it is important to take into account the 3D spatial distribution of the data that will be used for the estimation of the compensation parameters.

A. Performance analysis

The performance related to this method has been compared in terms of normalized root mean square error (NRMSE), evaluated as ratio between the RMSE and the Cramer-Rao bound (CRB), which represents the theoretical lower bound

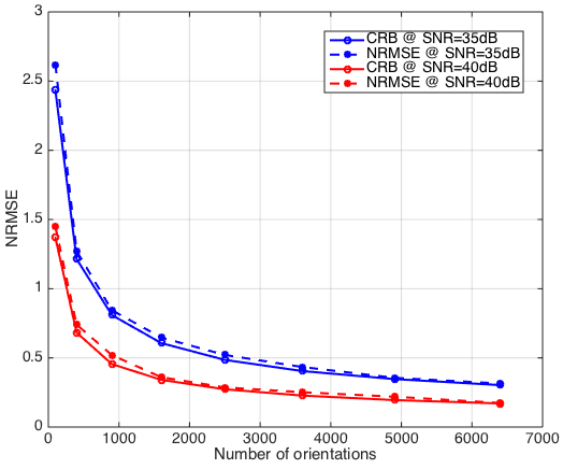

Fig. 2. Comparison between Cramer-Rao Bounds for the estimation of the nine model parameters and the NRMSE value obtained from non-linear ellipsoid compensation for numbers of 3D uniformly distributed orientations [100, 6500] at SNR values of 35 dB and 40 dB with $P = 1$.

on the standard deviation of the estimators for the model parameters. Both CRB and NRMSE values have been evaluated considering measurements provided at different orientations uniformly distributed in the 3D space. In particular, the CRB has been evaluated considering the root of the sum of the standard deviations for the estimation of each model parameter [11]. In Fig. 2, it is possible to see that the NRMSE values provided by the proposed compensation method approximate the CRB values. Furthermore, by increasing the number of orientations considered for the compensation procedure, the CRB decreases (see Fig. 2). By increasing the SNR value, the CRB and the NRMSE values of the compensation method decrease. Additionally, despite not being shown in Fig. 2, averaging the P samples acquired at each orientation decreases the NRMSE values related to the model parameters.

IV. The Real-Time Compensation Method

The proposed method consists of two steps: (i) a constant field compensation step, and (ii) a real-time compensation step. The first compensation step is performed using different orientations uniformly distributed in the 3D space and in environment with the magnetic field conditions kept constant. The even distribution is guaranteed using a 3-axis motorized stage that allows for the positioning of the sensor in several orientations. This 3-axis system keeps the smartphone in several fixed orientations for the time required by the acquisition of a limited number of samples of the magnetic field. The orientation of the 3-axis motorized stage is measured versus a reference orientation measurement system. The number of orientations used for this constant field compensation is 4000 and, for each orientation, one sample is considered. In this way, according to the obtained results (see Fig. 2), with an SNR of 35 dB, the NRMSE is around 40%.

The real-time compensation process can be described as a flowchart, as depicted in Fig. 3. In the variability evaluation stage, the procedure requires the evaluation of the standard deviations related to the elevation and azimuth angles using the model parameters evaluated in a previous step $\mathbf{M_k}$ e $\mathbf{b_k}$. In this case, the compensated measurements $\mathbf{h}$ are given by:

$$\mathbf{h} = \mathbf{M_k}^{-1}(\mathbf{h_m} - \mathbf{b_k}) \tag{11}$$

where $\mathbf{h_m}$ are the uncompensated measured values.

From these values, it is possible to estimate the elevation θ and azimuth ϕ angles, respectively:

$$\theta = \frac{180}{\pi} \cdot \arccos(h_z) \tag{12}$$

$$\phi = \frac{180}{\pi} \cdot \arctan 2(h_y, h_x) \tag{13}$$

where

$$\arctan 2(y, x) = \begin{cases} \arccos\left(\frac{x}{\sqrt{x^2+y^2}}\right) & \text{if } y \geq 0 \\ -\arccos\left(\frac{x}{\sqrt{x^2+y^2}}\right) & \text{if } y < 0 \end{cases} \tag{14}$$

The standard deviations for elevation and azimuth angles give a hint on the degree of the spatial distribution of the captured orientations and are evaluated over a window of measurements provided by the sensor that has a fixed size (e.g., 100 measurements). In order to obtain a good accuracy result in terms of estimated model parameters (see Fig. 2), the real-time compensation procedure should be performed on measurements with a uniform 3D spatial distribution. During the real-time compensation, the 3D spatial distribution is quantified using the following figure of merit:

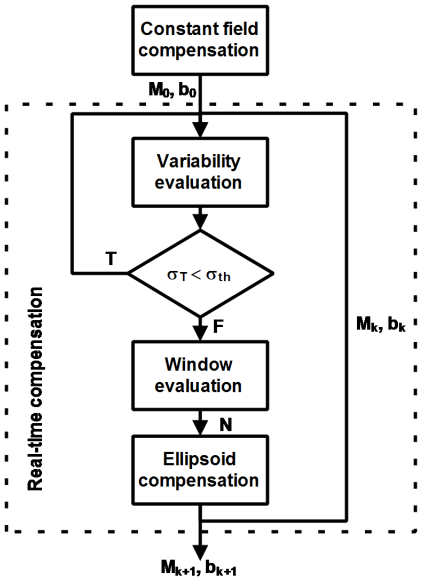

Fig. 3. The proposed compensation procedure.

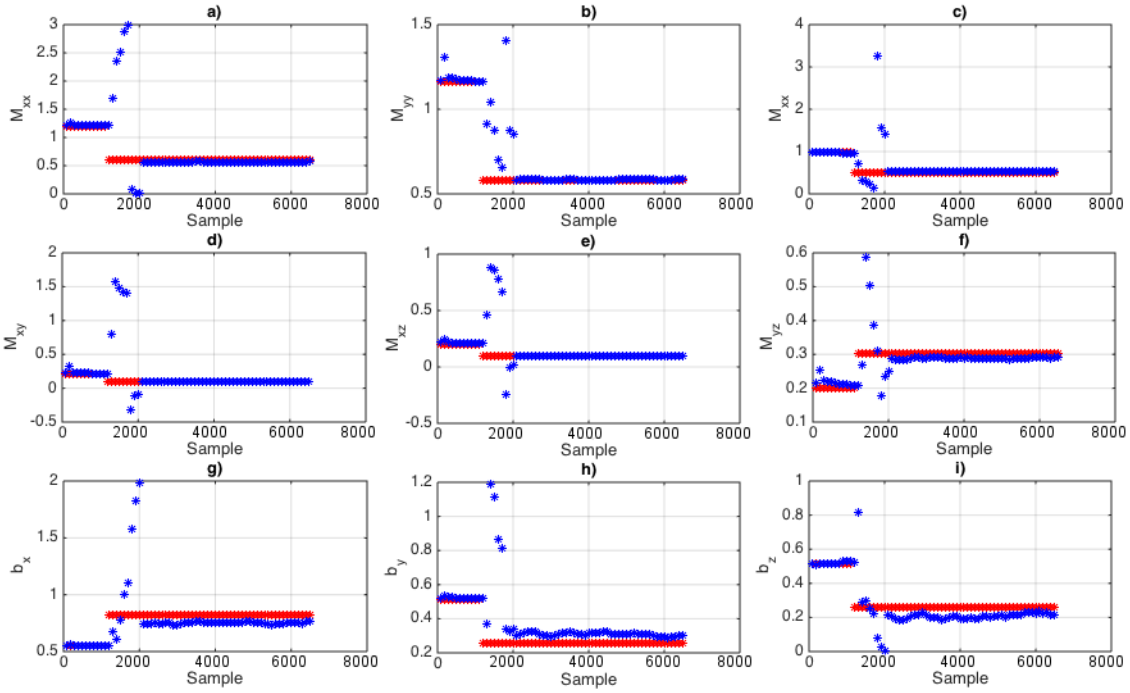

Fig. 4. The response of the proposed real-time compensation method considering a step variation of each model parameter, M_{xx}, M_{yy}, M_{zz}, M_{xy}, M_{xz}, M_{yz}, b_x, b_y, and b_z. The red markers represent the compensation values considered for each step variation and the blue markers refer to the values estimated by the proposed real-time compensation method.

$$\sigma_T = \sqrt{\sigma_\phi^2 + \sigma_\theta^2} \tag{15}$$

where σ_ϕ and σ_θ are the normalized standard deviations for azimuth and elevation angles, respectively.

If the spatial distribution of the orientations is even, the σ_T value will be about 1, meaning that it is possible to apply the method using only the measurements acquired over the N latest acquired orientations. On the other hand, if the σ_T value is low, the compensation will be performed by considering measurements acquired over a wider window (e.g., 2000 measurements) achieving and acceptable error (see Fig. 2). If the σ_T value is even lower than a threshold value σ_{th}, the real-time compensation will be not performed and the concerned data get discarded as the spatial distribution is not uniform. For this reason, in the window evaluation state, according to the figure of merit value σ_T, the value associated to the number of orientations used for the compensation step is evaluated with the following formula:

$$N = N_{max} - (N_{max} - N_{min})\sigma_T \tag{16}$$

where N_{max} and N_{min} are the maximum and minimum number of orientations considered for the real-time compensation, respectively. In this case, the number of orientations used for the compensation N can assume values within the range $[N_{min}, N_{max}]$. In the proposed compensation procedure, the N_{max} has been chosen equal to the number of orientations used in the constant field compensation step. N_{min} is equal to the number of orientations used for the standard deviation estimation. If the σ_T value is equal to 1, the number of orientations used for the compensation will be equal to the number of orientations used for standard deviation estimation. This is due to the fact that the acquired orientations have an even spatial distribution. In this case, the latest N_{min} samples are used for the ellipsoid compensation. Lower values of σ_T mean that the orientations used for the standard deviation estimation are not uniform, so the ellipsoid compensation has to rely on orientations referred to older instants. The last state of the proposed real-time compensation procedure is called ellipsoid compensation. The outputs of this state are the new compensation parameters estimated on the number of samples evaluated in the previous state, $\mathbf{M_{k+1}}$ and $\mathbf{b_{k+1}}$ according to (10).

V. Results

A first performance analysis of the proposed compensation method has been carried out considering several simulation tests. It is worth pointing out that the results shown in this Section have been obtained setting $P = 1$. This was to emulate real life conditions as the real-time compensation, unlike the constant field compensation, is supposed to happen while the smartphone is being operated by a roaming human subject, when it is not possible to guarantee that the sensor stays still to acquire $P > 1$ samples for each orientation. The magnetometer measurements have been simulated considering an additive white Gaussian noise for each axis signal in terms of signal-to-noise ratio (SNR) according to an ideal orientation of the smartphone. The SNR value considered in

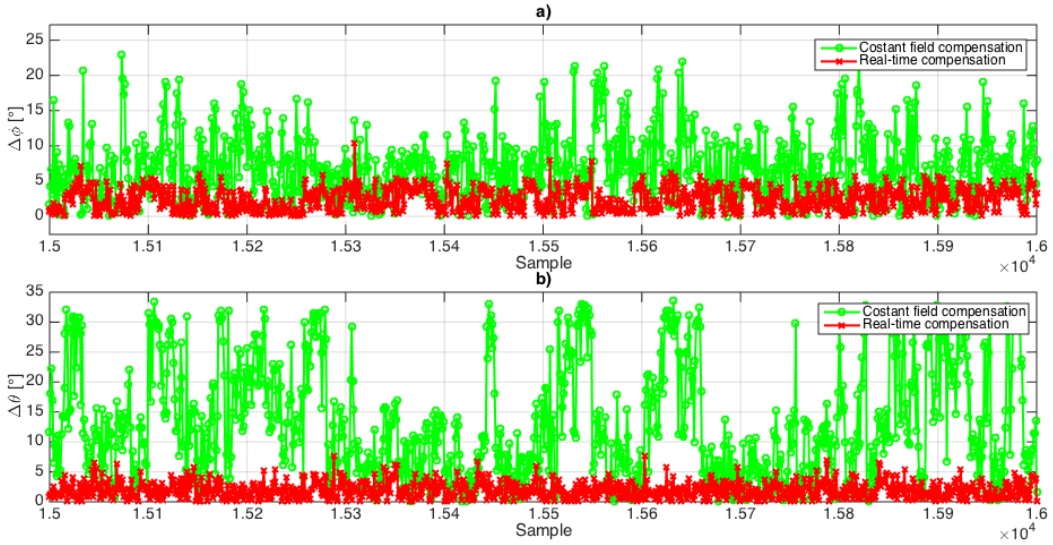

Fig. 5. Comparison in terms of azimuth and elevation angles errors between the angles evaluated using constant field compensation and the angles evaluated with the proposed real-time compensation method.

the simulation is 30 dB. During these tests, the disturbance has been simulated as a step variation of the model parameters, $\mathbf{M}$ and $\mathbf{b}$. The first test consists of analyzing the step response of the proposed compensation method considering the variation of the estimated parameters $\mathbf{M_{k+1}}$ and $\mathbf{b_{k+1}}$ respect to the known compensation parameters variations. In Fig. 4, the test results for each estimated parameter are reported. In this first simulation test, the considered step variations for each compensation parameter are the 50% of the initial compensation values. The variability evaluation is performed over 100 orientations. The window size N is set from 100 to 2000, according to the evaluated σ_T value. The obtained results show a transient of about 700 samples for each estimated parameter. Furthermore, for the offset parameters b_x, b_y, b_z and for the cross-axis compensation value M_{yx}, the steady state estimated values differ from the ideal values of about 20%.

In Fig. 5, the differences in terms of azimuth and elevation angles, from the values of angles estimated by considering the constant field compensation parameters and the real-time compensation parameters are depicted. The errors related to constant field compensation results for azimuth and elevation angles have peak values of 23° and 33°, respectively. On the other hand, the proposed algorithm proves to be able to respond promptly to changing conditions by limiting the errors for azimuth and elevation to 10° and 8°, respectively.

VI. Conclusion

In this paper a real-time method for magnetometer sensor output compensation is proposed. A description of the already used methods is reported and their disadvantages have been highlighted and discussed. The proposed method has been validated with preliminary simulation tests. Future works will be focused on: (i) improving the variability detection and the window evaluation steps considering a figure of merit that takes into account directly the spatial distribution so that only samples with a wide spatial distribution are used, (ii) implementing the algorithm on a smartphone, (iii) defining experimental validation, and (iv) performing it.

VII. Acknowledgment

This research was supported by the IEEE Instrumentation and Measurement Society 2015 Graduate Fellowship Award.

References

[1] P.Daponte, L.De Vito, F.Picariello, M.Riccio, “State of the art and future developments of measurement applications on smartphones”, J. of Measurement, Vol. 46, No. 9, Nov. 2013, pp. 3291-3307.

[2] C.Huang, S.He, Z.Jiang, C.Li, Y.Wang, X.Wang, “Indoor positioning system based on improved PDR and magnetic calibration using smartphone”, Proc. of IEEE 25th Annual Int. Symposium on Personal, Indoor, and Mobile Radio Comm., pp.2099-2103, 2-5 Sept. 2014.

[3] G.Retscher, T.Hecht, “Investigation of location capabilities of four different smartphones for LBS navigation applications”, Int. Conf. on Indoor Positioning and Indoor Navigation, pp.1-6, 13-15 Nov. 2012.

[4] P.Daponte, L.De Vito, S.Rapuano, M.Riccio, F.Picariello, “Compensating magnetic disturbances on MARG units by means of a low complexity data fusion algorithm”, Proc. of IEEE Int. Symposium on Medical Measurements and Applications (MeMeA), pp.157-162, 7-9 May 2015.

[5] 4. J.-H.Wang, Y.Gao, “A new magnetic compass calibration algorithm using neural networks”, J. of Measurement Science and Technology, Vol. 17, No. 1, 15 Dec. 2005.

[6] T.Beravs, S.Begus, J.Podobnik, M.Munih, “Magnetometer Calibration Using Kalman Filter Covariance Matrix for Online Estimation of Magnetic Field Orientation”, IEEE Trans. of Instrumentation and Measurement, Vol. 63, no. 8, pp. 2013-2020, Aug. 2014.

[7] Data sheet of LSM303DLH. Available online: www.st.com.

[8] V.Renaudin, M.H. Afzal, and G.Lachapelle, “Complete triaxis magnetometer calibration in the magnetic domain”, J. of Sensors, Vol. 2010, No. 967245, 2010.

[9] Paul D. Groves, “Principles of GNSS, Inertial, and Multisensor Integrated Navigation Systems”, Artech House, 1 Apr. 2013 2nd Edition.

[10] S.Bonnet, C.Bassompierre, C.Godin, S.Lesecq, A.Barraud, “Calibration methods for inertial and magnetic sensors”, J. of Sensors and Actuators Physical A, Vol. 156, No. 2, pp. 302-311, Dec. 2009.

[11] S.M.Kay, Steven M., “Fundamentals of statistical signal processing. Estimation theory”, Prentice Hall, Vol. I, 1993.